Analysis and Simulation of an Extended Data Set of Waveforms Received from Small Explosions in Shallow Oceans

Adrian D. Jones (1), Amos L. Maggi (2), Paul A. Clarke (1) and Alec J. Duncan (2)

(1) Maritime Operations Division, Defence Science and Technology Organisation, Australia, adrian.jones@dsto.defence.gov.au
(2) Centre for Marine Science and Technology, Curtin university of Technology, Australia, a.maggi@cmst.curtin.edu.au

ABSTRACT

DSTO possesses a data set of sound pressure time series received at a number of ranges from small explosive detonations along a number of tracks in shallow oceans in the Australian region. In recent years, these time series data have been under study by DSTO and Curtin University in relation to the potential impact of underwater explosions on marine fauna, in particular, marine mammals. Past work had shown that the characteristics of waveforms received at medium ranges might be simulated closely if bathymetry and sound speed data were known, and if the seafloor reflectivity was known at relevant frequencies. Sound pressure peaks were, however, over-predicted by the modelling, unless time spreading effects attributed to reflections from non-smooth ocean boundaries were included.

This paper reviews this past work and shows the results of more recent analyses in which data along a much greater number of ocean tracks have been studied. It does appear from this analysis of the extended data set that if the sound transmission from an explosive detonation is via bottom bounces, or via surface reflections from a rough surface, the peak level received is considerably less than the value expected from weak shock theory for a single arrival in a uniform ocean of infinite extent. However, if transmission is via surface reflections from a nearly smooth surface, the measured peak level is closer to the theoretical value. This conclusion is illustrated with a presentation of at-sea data and comparison with modelled time series.

INTRODUCTION

The Australian Defence Force (ADF) has a strong commitment to conduct its maritime operations and training activities in a manner which is environmentally responsible. A relevant issue is the radiation of acoustic energy in the undersea environment. This may occur as a bi-product of general at-sea activity (for example, a ship at sea will radiate machinery sounds underwater), will result from the use of active sonar systems and echo-sounders, and will result from the underwater detonation of explosives. A particular type of small explosive which has been used in the past by the ADF is the Signal Underwater Sound, otherwise known as SUS charge (see, for example, Urick, 1983). In order to be able to advise the ADF of the environmental implications of the use of SUS charges, and to gain an insight into the environmental issues associated with explosives in general, DSTO in conjunction with Curtin University, has been conducting related research. This paper reviews the present progress of this work.

Previous Work

In previous work (Jones and Clarke 2004, 2005 and Jones, Duncan, Clarke and Maggi 2005), sound pressure peak data received along three separate shallow ocean tracks were presented. Data for each of these tracks (Tracks A, B and C) showed a substantial difference between the peak level predicted by established weak shock theory for a quiescent ocean of infinite extent (Rogers 1977) and the observed peak level. These differences were of the order of 12 to 20 dB, with the measured peak being less than the value predicted at the same range.

In each case, the broadband acoustic signal energy level was within expected limits. Further, simulations of the time series events, which were carried out using the SCOOTER and BELLHOP transmission models combined in a transform function method, showed that general waveform features were well followed but the peaks were greatly over-predicted (Jones, Duncan, Clarke and Maggi 2005) relative to at-sea data. An attempt at including ray-path time-spreading in the modelling brought the predicted peak levels closer to the measurement, and the authors speculated that some such time spreading phenomena may indeed be occurring.

The data for Tracks A, B and C were all obtained for essentially downward refracting scenarios, for which direct path transmission was not possible to ranges for which data was held, and thus all arrivals encountered at least one bottom bounce. Further, the prevailing ocean conditions were in the order of sea state 1 (on-site wind speed was 4 to 5 kt, swell height 0.1 m) or less, so that surface effects would be minimal. It thus occurred to the authors that there was the possibility that a time spreading phenomenon was occurring either in water-borne transmission, or upon bottom interaction.

Recent Work

In recent work, received SUS data for a further twelve tracks in shallow ocean regions have been examined closely. For four of these additional tracks (Tracks Q, R, T and V), the ocean was uniformly upward refracting with a gradient approximating isothermal conditions. For an additional track (Track H), the ocean contained an upward refracting surface duct to a depth of 55 m - again, the gradient approximated isothermal conditions. For three of these five tracks, the wind speed and sea state were quite low, and for the other

two tracks, the wind speed and sea state were much higher. These data offered the opportunity to investigate whether time spreading phenomena were evident in transmission dominated by upward refraction and repeated surface skips, and whether any noticeable difference was caused by surface roughness.

For two of the additional tracks (Tracks E and N), the sound speed gradient was downwardly refracting to a depth well beyond the 18.3 m at which the SUS charges were detonated and the receivers located. These data offered the opportunity to confirm the conclusions from earlier work by the authors (Jones, Duncan, Clarke and Maggi 2005) that a large reduction in received peak level would occur.

The remaining five tracks were for ocean environments for which the sound speed variations with depth could not be readily classified as either upwardly or downwardly refracting. Those data have not been considered further in what is reported below.

FEATURES OF DATA COLLECTION

For each track, the data were obtained using a suitable receiver located at 18.3 m depth from a surface buoy, while SUS charges were deployed from a ship as it moved away. Each SUS charge was set to detonate at 18.3 m depth. Typically, source to receiver range values were not less than several kilometres, and extended to the order of 20 kilometres. Ocean depths were obtained continuously along the tracks using a ship-based high-frequency echo sounder, and were found to be uniform to a reasonable approximation along each track, and were the order of 100 m or less. Surficial sediment samples were obtained at the start of each track. At least two bathythermograph recordings were made for each track, from which sound speed variation with depth was determined. Due to the shallowness of the ocean environments, refraction in transmission had the effect that no direct path arrival was received at source to receiver ranges for which valid recordings were made. Each received waveform consisted of a burst of signal arrivals resulting from the high number of surface and bottom bounces.

Time series of sound pressure arrivals were selected for analysis only for those waveforms for which the measured peak excursion pressure was at least 5.5 dB less than the hard-clipping limits of the recording system used for each track. Here, the recording system specifications accounted for individual sonobuoy characteristics. This criterion was chosen as it exceeded the maximum possible amount by which the assumed waveform of the initial peak (an instantaneous rise, followed by an exponential decay with time constant about 0.1 ms) might be underestimated due to the digital sampling rate of 20 kHz, and anti-alias filtering at 8 kHz, which were employed. A simulation of the data sampling and anti-alias filtering showed that the average "missing of the peak" would be about 3 dB for a pressure peak of ideal form. If a small amount of time spreading was imposed on the initial peak by the ocean environment, the data acquisition system would have been even more able to follow the true peak waveform. Data collected on-site did not include any information which might be used to determine the extent of any time spreading in the in-water transmission.

DOWNWARD REFRACTING ENVIRONMENTS

The key data for all five downward refracting environments are summarised in Table 1. Here, the reported measured peak value is the largest sound pressure excursion, positive or negative, over the entire duration of the received sound pressure waveform. The value described as "theoretical" is that predicted at that range by weak shock theory (Rogers 1977). The latter, of course, assumes a uniform quiescent ocean of infinite extent. Both these values are broadband, in the sense that no frequency-selective filtering of the data has occurred. The difference, or "Δ" between the measured and theoretical values is shown in dB form.

Table 1. Measured and predicted received SUS sound pressure data for shallow water tracks with downward refraction

Ocean Track	Range (km)	Measured peak (Pa)	Theoretical Peak (Pa)	Δ dB
Track A	5.10	268	1490	14.9
	10.1	146	732	14.0
Track B	3.51	319	2200	16.7
	5.05	161	1500	19.3
	10.7	58	690	21.5
Track C	5.58	345	1350	11.8
	10.7	114	690	15.6
Track E	3.55	352	2163	15.8
	5.31	286	1426	14.0
	10.2	110	723	16.4
Track N	7.70	128	970	17.6
	11.8	95	621	16.3
	16.1	29	451	23.8

On-site data relating to these tracks, and to the conditions prevailing at the ocean surface during the conduct of the measurements along these tracks, are shown in Table 2. Clearly, a consistent feature is the relatively low sea state and smooth ocean surface conditions. This is to be expected, as downward refraction at the surface will result from prolonged solar heating in the absence of surface movement.

Table 2. Ocean depth and sea surface data for shallow water tracks with downward refraction

Ocean Track	Ocean depth (m)	Wind speed (m/s)	Swell height (m)
Track A	58 - 65	1	0
Track B	89 - 95	2.5	0.1
Track C	62 - 51	2	0
Track E	63	4	0
Track N	110 - 100	0	0

Track A

A ray diagram prepared for Track A using the BELLHOP model is shown in Figure 1 (data for Tracks B and C are not shown in this paper). This has been prepared to include those rays launched at elevation angles commencing at 0.0 degrees and at 0.5 degree increments to ± 2½ degrees.

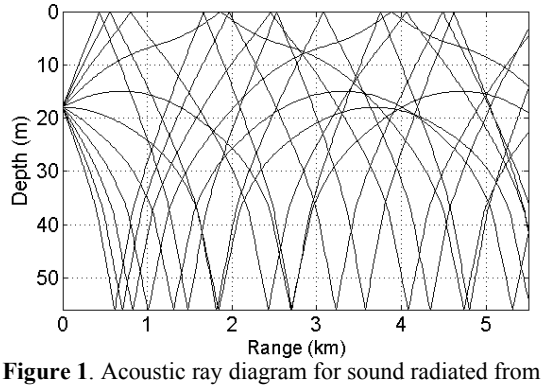

Figure 1. Acoustic ray diagram for sound radiated from source for Track A, 11 rays over ± 2½ degrees

The measured waveform received at 5.1 km is shown below in Figure 2. The detail of the initial part of the waveform is

shown in Figure 3. The peak pressure value reported in Table 1 was obtained from these data.

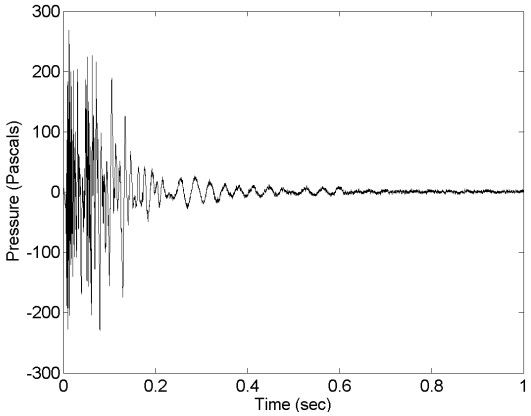

Figure 2. Received sound pressure time series, Track A, full pulse, 5.1 km

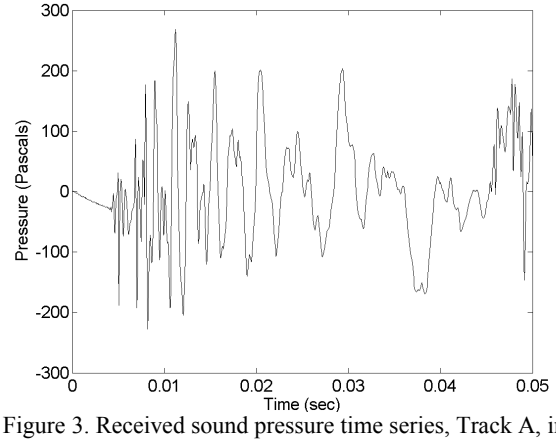

Figure 3. Received sound pressure time series, Track A, initial 0.05 s, 5.1 km

As described in earlier work by the authors (Jones, Duncan, Clarke and Maggi 2005), the SUS waveform received at 5.1 km range for Track A was simulated by generating an inverse Fourier transform of the product of the oceanic transfer function and the Fourier transform of the assumed input SUS waveform. The oceanic transfer function was based on the models SCOOTER (fast-field model) at low frequencies and BELLHOP (gaussian beam ray model) at remaining frequencies.

The Track A environment (Jones and Clarke 2004) was modelled using a uniform depth of 56.5m and assuming a sediment surface of fine silt to a layer depth of 259 m. The remainder of the substrate was treated as a limestone halfspace. The sound speed profile measured at the start of the track (Jones and Clarke 2004) was used for modelling the water column. The seafloor reflectivity implied by this assumed seabed is very close to that obtained for the same track by an acoustic inversion analysis applied to *in-situ* data (Jones et al 2002), hence we may be confident that the seafloor is well modelled in this process.

Measured and simulated time series waveforms for a receiver at 5.1 km along Track A are shown in Figure 4. This shows the leading edge detail of the time series data. These figures are reproduced from earlier work (Jones, Duncan, Clarke and Maggi 2005) and are shown here as an example of a simulation for a downward refracting environment.

The peak pressure excursion in these simulations is 1413 Pa. This is quite close to the peak value of 1490 predicted from weak shock theory, and shown in Table 1. It has been shown by the authors (Jones, Duncan, Clarke and Maggi 2005) that the peak value from a simulation of the waveform at 10.1 km range is 498 Pa, which is close to the theoretical value of 732 Pa shown in Table 1.

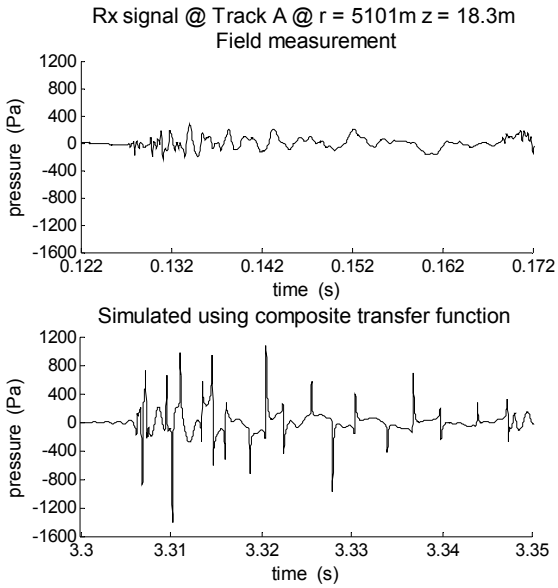

Figure 4. Measured & simulated waveforms, 5.10 km, Track A – detail of initial pulse

Tracks E and N

For Tracks E and N, the measured time series data and ray diagram calculations are shown below in Figures 5 to 10.

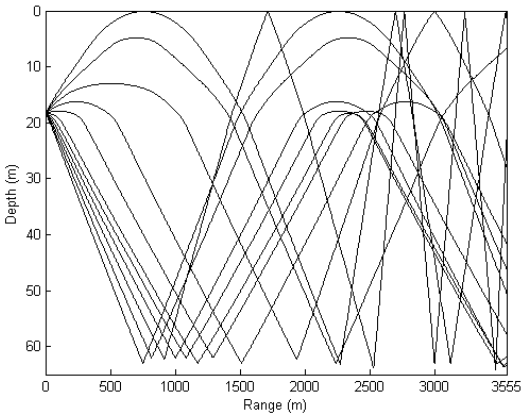

Figure 5. Acoustic ray diagram for sound radiated from source for Track E, 11 rays over ± 2½ degrees

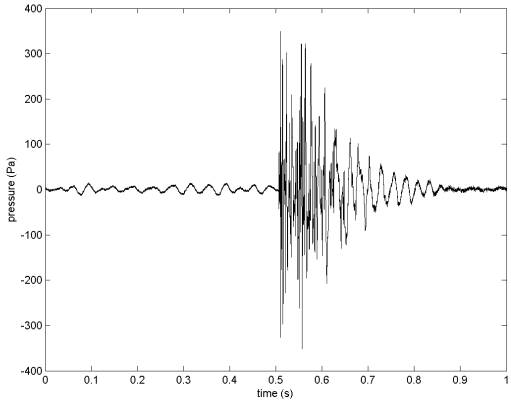

Figure 6. Received sound pressure time series, Track E, full pulse, 3.6 km

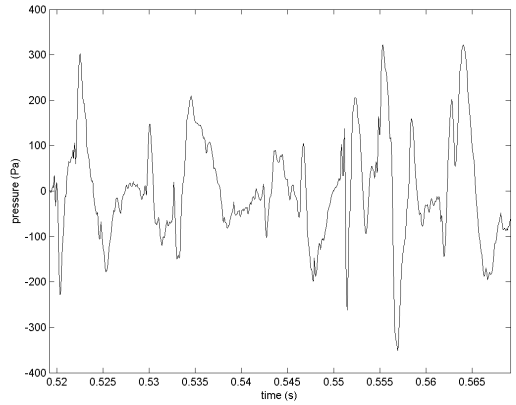

Figure 7. Received sound pressure time series, Track E, initial 0.05 s, 3.6 km

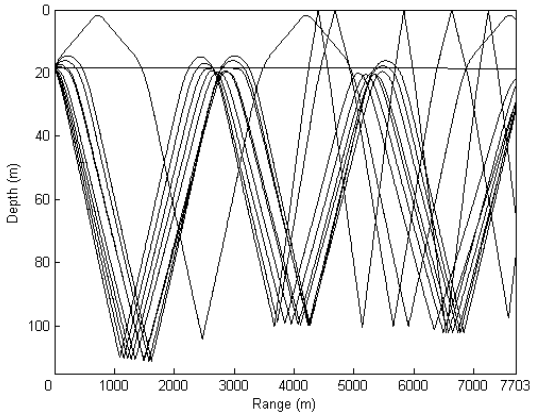

Figure 8. Acoustic ray diagram for sound radiated from source for Track N, 11 rays over ± 2½ degrees

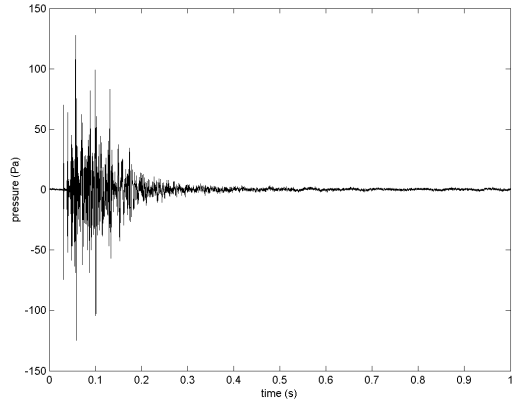

Figure 9. Received sound pressure time series, Track N, full pulse, 7.7 km

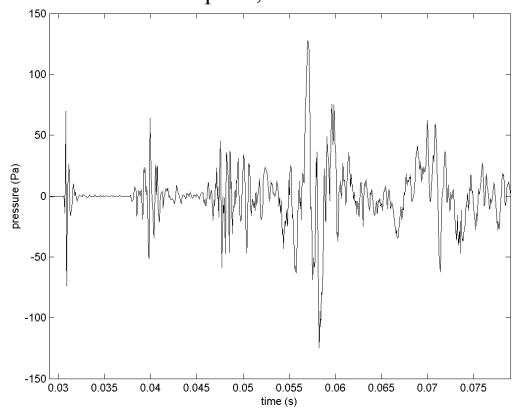

Figure 10. Received sound pressure time series, Track N, initial 0.05 s, 7.7 km

Time series simulations have yet to be completed for Tracks E and N.

Discussion – downward refracting environments

For each of the Tracks A, E and N, the downward nature of the refraction is quite pronounced. From inspection of the ray diagrams in Figures 1, 5 and 8, signals received at a depth of 18.3 m at the ranges shown in Table 1 must encounter a number of bottom bounces. The minimum number of bottom bounces for transmitted rays, and the observed seafloor roughness are shown in Table 3. These roughness values were derived as the standard deviation from a straight line of best fit to the continuous bathymetry data which was recorded along each track. The surficial sediment data at the start of each track are also shown in Table 3.

Table 3. Minimum number of bottom bounces in transmission to first point along tracks - downward refraction

Ocean Track	Minimum no.bottom bounces	rms Bottom Roughness (m)	Surficial sediment
Track A	1	2.19	fine silt
Track B	1	1.24	medium sand
Track C	2	2.64	coarse silt
Track E	1	0.72	coarse – medium silt
Track N	3	5.0	shelly sand

The time series data received at the first point along each track, shown in Figures 2, 6 and 9, have a characteristic shape. There is no single dominant arrival in the case of any of these time series, and there is a complex waveform of total duration about 0.5 seconds or less. The detail of the start of each pulse is shown in Figures 3, 7 and 10. These confirm the lack of a single dominant arrival.

The simulated data in Figure 4 suggests an over-prediction, however, close inspection shows that, apart from the magnitude of the sharp peaks, the simulated time series is accurate in estimating the duration, amplitude and character of the features of the waveform. The peak amplitude of the simulated data is much greater than the measured peak, and the largest peak excursion (1413 Pa) is very close to a theoretical value based on weak shock theory for direct arrivals (1490 Pa). In earlier work (Jones and Clarke 2004, 2005) it was suggested that peak values associated with such short duration impulses might be spread in time, slightly, due to non-specular reflections from boundaries and/or due to thermal microstructure effects. Any such time spreading would result in some reduction of peak values. An attempt was made to simulate the existence of such transmission along a number of micro-paths connecting the transmitter and receiver, each with a slightly different transmission delay (Jones, Duncan, Clarke and Maggi 2005). The results of this initial simulation was indeed a reduction of peak values to observed levels, however, the degree to which this occurred was very much dependent on the choice of parameters for the simulation. Those simulations, not shown here, did suggest that some form of micro-path phenomena might be occurring, however it was considered more useful to examine more at-sea data prior to any detailed study of the phenomenon.

For Track A, the fact that the sampled sediment was fine silt, for which the mean grain size was determined as $\phi = 6.4$ (ϕ is related to grain diameter, d, millimetres, as $\phi = -\log_2 d$), may suggest that a high bottom loss is expected and that the received pressure is simply reduced in amplitude in accord to the bottom losses. However, for the case in question, the grazing angles of relevant arrivals are quite small, so that the bottom losses for these arrivals are small. In fact a simulation of bottom loss versus grazing angle for the modelled seafloor, shown in Figure 8 of Jones, Duncan, Clarke and

Maggi (2005) shows a reflection coefficient in excess of 0.9 (less than 1 dB bottom loss) for grazing angle of 5 degrees, which corresponds with most of the rays depicted in Figure 1. Critical angle for the seafloor as modelled for Track A is at about 12 degrees, above which angle the reflection coefficient falls to about 0.3 (bottom loss 10 dB). All relevant arrivals, however, are incident on the seafloor at angles much less than critical angle.

A simple conclusion from these data is that a reduction in peak level for an explosive impulse, relative to the expectation from weak shock theory, occurs if the received signal travels via a number of bottom bounces in a downward refracting environment. A more elaborate conclusion, however, cannot be drawn from these data.. In the case of each track, data in Table 2 shows that the sea state was slight and the ocean surface was much more smooth than the seabed, for which roughness is indicated in Table 3. Although a large reduction in the peak value is shown in the data at all range points for all these tracks, the magnitude of the reduction is, however, not seen to be dependent upon bottom roughness or on the number of bottom bounces. In particular, the peak reduction for Track E is similar to that for Track N regardless of the fact that Track E has the lowest value of seafloor roughness and only one bottom bounce, and for Track N the roughness is greatest and at least three bottom bounces exist. The authors have no explanation for this observation. It may be speculated that the strength of the downward gradients (averaging – 0.15 m/s per m in a few cases) is a factor, as this will result in bottom interactions all being at appreciable angles of incidence (about 4 to 5 degrees minimum).

UPWARD REFRACTING ENVIRONMENTS

The key data for all five upward refracting environments are summarised in Table 4. The reported measured peak value is the largest sound pressure excursion, positive or negative, over the entire duration of the received sound pressure waveform. The value described as "theoretical" is that predicted at that range by weak shock theory (Rogers 1977). The difference, or "Δ" between the measured and theoretical values is shown in dB form.

Table 4. Measured and predicted received SUS sound pressure data for shallow water tracks with upward refraction

Ocean Track	Range (km)	Measured peak (Pa)	Theoretical Peak (Pa)	Δ dB
Track H	15.7	287	463	4.1
Track Q	13.2	317	555	4.9
	15.2	312	480	3.7
	17.1	304	424	2.9
Track R	9.7	653	764	1.4
	11.8	573	623	0.7
	13.7	476	536	1.0
Track T	17.5	128	414	10.2
	20.4	129	353	8.7
Track V	17.0	144	427	9.4
	19.3	144	374	8.3
	21.5	113	336	9.5

On-site data relating to these tracks, and to the conditions prevailing at the ocean surface during the conduct of the measurements along these tracks, are shown in Table 5. The stated ocean depth values are averages for each track. For Tracks H, Q and R, the sea state was quite low, whereas for Tracks T and V the sea state was higher and the sea surface was rough.

Table 5. Ocean bottom and sea surface data for shallow water tracks with downward refraction

Ocean Track	Ocean depth (m)	rms Bottom Roughness (m)	Wind speed (m)	Swell height (m)
Track H	87	3.0	2.5 – 3.5	1
Track Q	64	3.1	4 - 5	0.5
Track R	66	0.7	1.5 – 2.5	0.25
Track T	79	3.1	14 - 18	2
Track V	42	0.8	13.5	2

Tracks Q and R – smooth ocean surface

Data for Track H are not shown in this paper. For Tracks Q and R, the measured time series data and ray diagram calculations are shown below in Figures 11 to 16.

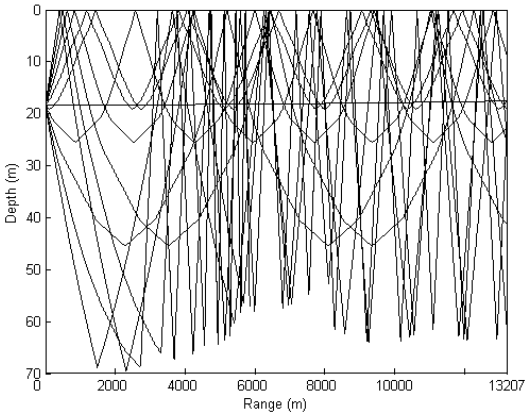

Figure 11. Acoustic ray diagram for sound radiated from source for Track Q, 11 rays over ± 2½ degrees

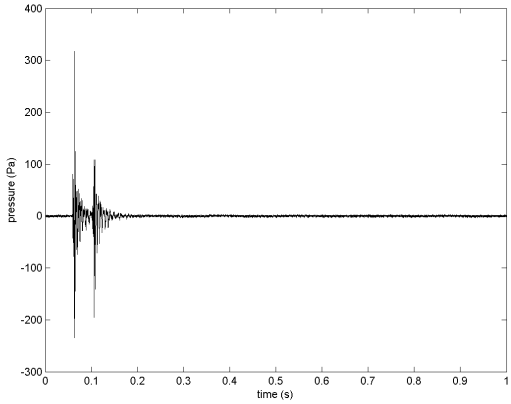

Figure 12. Received sound pressure time series, Track Q, full pulse, 13.2 km

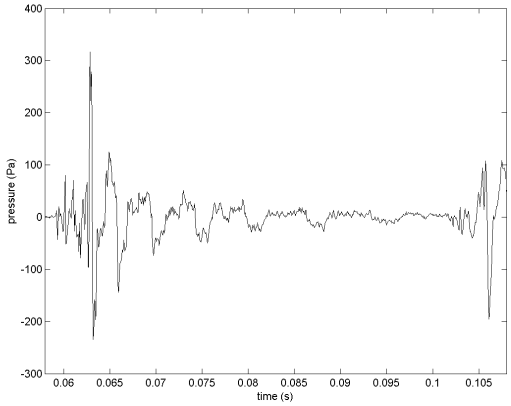

Figure 13. Received sound pressure time series, Track Q, initial 0.05 s, 13.2 km

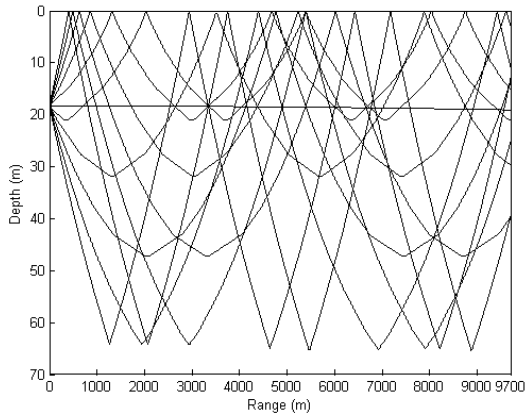

Figure 14. Acoustic ray diagram for sound radiated from source for Track R, 11 rays over ± 2½ degrees

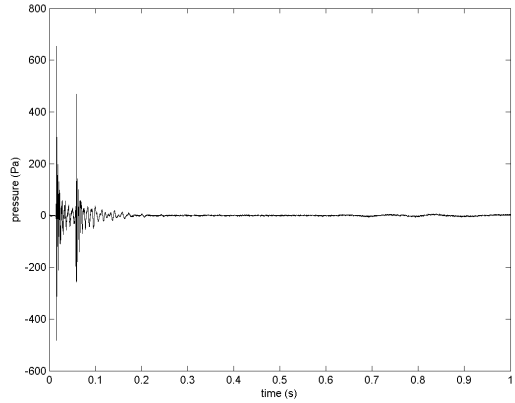

Figure 15. Received sound pressure time series, Track R, full pulse, 9.7 km

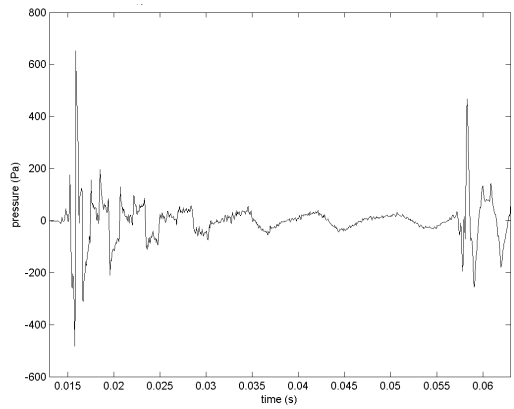

Figure 16. Received sound pressure time series, Track R, initial 0.05 s, 9.7 km

The SUS waveform received at 9.7 km range for Track R was simulated using the BELLHOP model. Here, an inverse Fourier transform of the product of the oceanic transfer function and the Fourier transform of the assumed input SUS waveform was generated. The environment was modelled using a uniform ocean depth of 67 m and assuming a sediment of sand, of thickness 259 metres, overlaying a half-space of sand. The compressional speed throughout the sediment, and half-space, was assumed 1650 m/s. The shear speed in the sediment was modelled as 110 m/s at the seabed, increasing to 582 at the boundary with the half-space. Compressional and shear attenuations were modelled as 0.8 dB/wavelength and 2.5 dB/wavelength, respectively, throughout sediment and half-space. The sound speed profile measured at the start of the track was used for modelling the water column. A uniform sand sediment and substrate was chosen, as surficial sediment data indicated 98% sand and no other determination was available. The leading edge data for measured and simulated time series waveforms are shown in Figure 17, where the data from Figure 16 is repeated for convenience of comparison. Note that the simulated result has been low-pass filtered above 8 kHz, so that this might match the filtering of the at-sea data by the anti-alias filter.

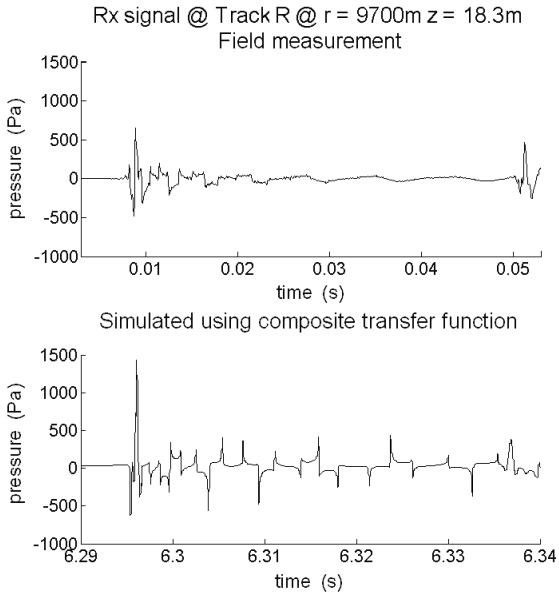

Figure 17. Measured & simulated waveforms, 9.7 km, Track R – detail of initial pulse

The peak pressure excursion in these simulations is 1368 Pa. This is greater than the peak value of 764 predicted from weak shock theory, and shown in Table 4, and exceeds the measured peak vale of 653 Pa by 6.4 dB.

Time series simulations have yet to be completed for Tracks H and Q.

Track V – rough ocean surface

Data for Track T are not shown in this paper. For Track V, the measured time series data and ray diagram calculations are shown below in Figures 18 to 20.

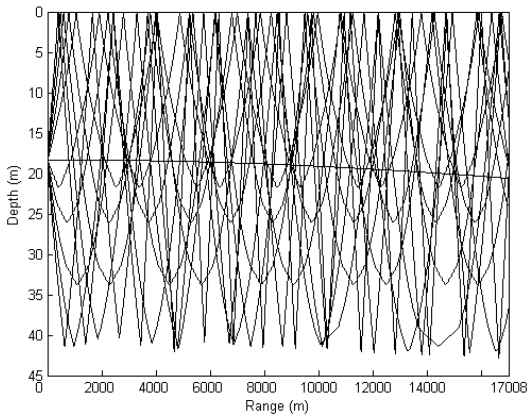

Figure 18. Acoustic ray diagram for sound radiated from source for Track V, 11 rays over ± 2½ degrees

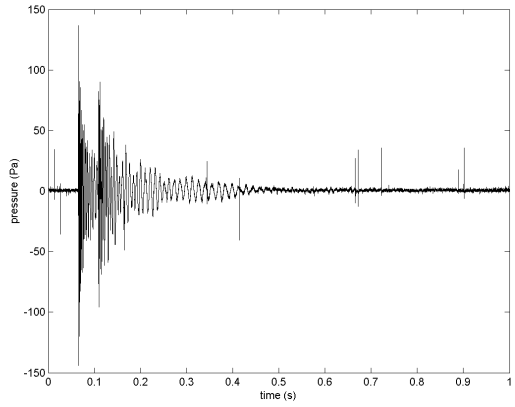

Figure 19. Received sound pressure time series, Track V, full pulse, 17.0 km

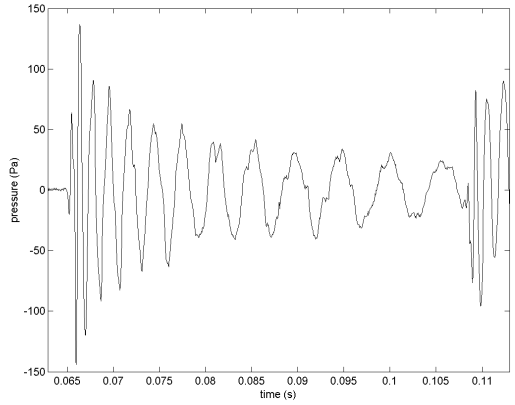

Figure 20. Received sound pressure time series, Track V, initial 0.05 s, 17.0 km

Time series simulations have yet to be completed for Tracks T and V.

Table 6. Minimum number of surface skips in transmission to first point along tracks - upward refraction

Ocean Track	Depth of upward refracting layer (m)	Minimum no. surface skips	Average sound speed gradient (m/s per m)
Track H	55	2	0.011
Track Q	64 (to seabed)	2	0.018
Track R	66 (to seabed)	1	0.02
Track T	45	3	0.022
Track V	42 (to seabed)	5	0.032

Discussion – upward refracting environments

For each of the Tracks Q, R and V, the upward nature of the refraction is quite pronounced. From inspection of the ray diagrams in Figures 11, 14 and 18, signals received at a depth of 18.3 m at the ranges shown in Table 4 travel either via repeated surface skips or encounter a large number of bottom bounces. From the ray diagrams, the minimum number of surface skips to the first range point along these tracks is indicated in Table 6. The table also shows the depth from the ocean surface to the bottom of the upward refracting layer. In the case of Tracks Q, R and V, the sound speed gradient is upward refracting for the entire ocean depth. For Track H the gradient was upward refracting to a depth of 55 m, whereas for Track T, the zone of upward refraction extended from the surface to 45 m depth. In the case of each ocean track, the average gradient within the upward refraction zone was more or less uniform, with these gradients shown in Table 6. Gradients for Tracks Q, R and T are similar to those resulting from isothermal conditions (0.017m/s per m, eg. as shown by Etter 1996), whereas the gradient for Track V is more pronounced. It may be shown that these numbers of minimum surface skips are consistent with standard expressions for surface ducts (eg. Etter 1996). It is worth noting, that for isothermal conditions, the grazing angle at the surface for a limiting ray in a duct of 45 m depth may be shown to be 1.8 degrees, and for a 60 m duct it is 2.1 degrees. Clearly, sound travelling by upward refraction and surface skips interacts with the surface at very shallow angles.

The time series data received at the first point along each of Tracks Q and R, shown in Figures 12, and 13, 15 and 16, respectively, have a similar characteristic shape. In each case, there exists a single dominant arrival and a second noticeable peak at a delay of about 0.04 seconds. This second peak may be recognised as the first bubble pulse, which is a well known phenomenon for SUS signals (eg. Hannay and Chapman 1999, Chapman 1988). In fact, the consistency of delay of the bubble pulse was used as a measure of the correctness of detonation of each particular explosive charge, and each observed delay was found to be well-matched to that expected for the particular charge weight and detonation depth.

For each waveform, there is a decaying burst of signal immediately after both the initial peak and the bubble peak. These waveforms are quite different in character from those of the downward refracting environments, shown earlier, in that these present waveforms exhibit a well-defined initial peak and bubble pulse peak, whereas, for the former, these peaks are by no means as pronounced.

The data for Track V, Figures 19 and 20, have an appearance which is similar to that for Tracks Q and R, however, the peaks are less pronounced relative to those components of the waveform due to higher order multi-path arrivals.

A notable feature of the data for Tracks Q and R is the fact that the observed peak levels are very close to those expected from weak shock theory. From the data in Table 6 it is apparent that, from a ray transmission consideration, acoustic energy may reach the receiver at the first range point with no bottom interaction and with, merely, two surface reflections (Track Q) or one surface reflection (Track R). Data in Table 5 shows that the sea state was low in each of these cases, so that all surface reflections were from relatively smooth surfaces. These data suggest that time spreading phenomena is not evident, or evident to a small degree only, for Tracks Q and R). In fact, it is noteworthy that the minimum difference, Δ, in the peak data of Table 4 is for Track R for which a ray arrival with just one surface bounce and no bottom bounces, exists, and for which a very low sea state exists (Table 5).

The data in Table 4 for Tracks V and T indicate that either a roughened sea surface, and/or a greater number of surface bounces increases the difference between an observed peak level and the peak level expected from weak shock theory. It would then appear that a time spreading, due to micro-path phenomena may be occurring in these cases.

The simulated data in Figure 17 are quite close to the measured data in terms of the general character of the waveform, however, there appears to be an over-prediction for the initial peak, and for the peaks associated with higher order arrivals. An examination of the BELLHOP output data shows that the initial peak is associated with a pair of arrivals separated in time by less than 0.02 ms. These arrivals each contribute a significant amplitude and are of identical phase. Their time separation is much less than the SUS waveform time constant (time for an instantaneous rise to decay by 1/*e*) of about 0.11 ms (Jones and Clarke 2004), and so it does appear that a coincident pressure summation is responsible for the peak

amplitude being about double that expected by weak shock theory. The BELLHOP output data also shows that arrivals received later than just 1.3 ms after the start of the pulse have at least two bottom bounces, and arrivals after 0.012 seconds have at least 5 bottom bounces and are incident on the bottom at angles of 4 degrees or more. Based on our earlier examination of downward refracting environments, for which incidence at the seafloor was of the order of 4 to 5 degrees or more, we then expect the peak data in all but the first 0.012 seconds of the waveform to be greatly reduced by time spreading on bottom interaction. With this consideration of the simulation in Figure 17, including a chance coincident summation of two arrivals, and our understanding that the simulation has not reduced the peak levels of higher order arrivals which would surely have encountered such a reduction, it does appear that the measured waveform is consistent with the simulation. In particular, the peak value of the measured data is consistent with the supposition that time spreading along the initial peak is not occurring to a significant degree, for this case of upward refraction to a relatively smooth ocean surface.

DISCUSSION

The measured data presented above are consistent in showing that, for downward refracting environments for which a transmitted signal impacts with the seafloor, peak levels received from SUS detonations in shallow ocean regions are much less than the expectation from weak shock theory. All the three tracks examined previously by the authors (Jones and Clarke 2004, 2005 and Jones, Duncan, Clarke and Maggi 2005) were essentially downward refracting. Two additional tracks (Tracks E, N), for which data is presented above, are also essentially downward refracting and exhibit the same large reduction in peak values. This reduction in peak values appears to be of the order of 15 dB regardless of the bottom roughness and number of bottom bounces. It is anticipated that this reduction in peak level is due to a time spreading phenomenon.

Data for environments with relatively smooth ocean surfaces and significant upward refraction (Tracks H, Q, R) show very little reduction (less than 5 dB) in peak values from expectation from weak shock theory. There is evidence in the data to suggest that this reduction appears to be increased as the number of surface skips in transmission increases and the sea state becomes higher.

Data for environments with significant upward refraction but a higher sea state (Tracks T and V) show a medium level of peak reduction (about 10 dB). This may be due to differences in surface reflection losses at high frequencies, or due to increased time spreading from reflections from the rougher ocean surface, or increased time spreading due to the fact that the near-surface part of the ocean is in a greater state of motion. It appears that all these three phenomena are minimised with a smooth ocean surface.

In all cases in which measurements were obtained along tracks exhibiting downward refraction (Tracks A, B, C, E and N), the sea was close to flat calm conditions. This is to be expected, as downward refraction at the surface is due to prolonged solar heating in the absence of surface movement. The results for upward refracting environments suggest that for a low sea state there is minimal occurrence of losses of any kind, so we may speculate that within a calm ocean with downward refraction there is no time spreading at the surface or within the water column. It then appears that the phenomena causing the large reduction in the peak for these downwardly refracting environments is a time spreading or a high frequency reflection loss on bottom bounces, only.

CONCLUSIONS

Received SUS waveform data have been examined for a significant number of shallow ocean tracks, and a consistent picture is emerging. In the analysis carried out in this study, it does appear that if the sound transmission from a SUS explosive detonation is via bottom bounces in a downward refracting environment, the peak level received is considerably less (difference about 15 dB) than the expectation from weak shock theory for a uniform ocean of infinite extent. This appears to be unrelated to the number of bottom bounces, and to the observed bottom roughness. However, if transmission is via surface reflections in an isothermal environment with a nearly smooth surface, the measured peak level is close to the theoretical value; if the surface is rough the measured peak is about 10 dB reduced.

ACKNOWLEDGEMENT

The authors acknowledge the efforts of those DSTO staff members who collected, processed and archived the data used in this paper.

REFERENCES

Chapman, N. R., 1988, *Source levels of shallow explosive charges*, J. Acoust. Soc. America, Vol. 84, No. 2, pp 697 – 702

Etter, Paul C., 1996, "Underwater Acoustic Modelling: Principles, Techniques and Applications", 2nd edition, E & FN Sponl

Hannay, D. E. and Chapman, N. R., 1999, *Source levels for shallow underwater sound charges*, J. Acoust. Soc. America, Vol. 105, No. 1, pp 260 – 263

Jones, A.D. and Clarke P.A., 2004, *Underwater Sound Received from some Defence Activities in Shallow Ocean Regions*, Proceedings of ACOUSTICS 2004, Gold Coast, Australia, pp 467 – 473

Jones, A.D. and Clarke, P.A., 2005, *Peak Levels from SUS Measured in Shallow Oceans in the Australian Region*, Intl. Conf. on Underwater Acoustic Measurements: Technologies and Results, Heraklion, Crete

Jones, A.D.; Duncan, A.J.;Clarke, P.A. and Maggi, A., 2005, *Simulation of Time Series Received Underwater from Small Explosive Detonations in Shallow Ocean Regions*, Proceedings of ACOUSTICS 2005, 9-11 November 2005, Busselton, Western Australia, pp 467 – 474

Rogers, P.H., 1977, *Weak-shock solution for underwater explosive shock waves* J. Acoust. Soc. America, Vol. 62, No. 6, pp 1412 – 1419

Urick, R.J., 1983, *Principles of Underwater Sound*, 3rd edition, McGraw-Hill